DOI: 10.1002/ejic.200800255

A Ferromagnetically Coupled Diiron(III) Complex with a *m*-Phenylenediamine-Based Ligand

Biplab Biswas,[a] Sunita Salunke-Gawali,[a] Thomas Weyhermüller,[a] Vinzenz Bachler,[a] Eckhard Bill,[a] and Phalguni Chaudhuri*[a]

Keywords: Iron / Diferric complexes / Schiff bases / Ferromagnetism / Spin polarization

The Schiff base ligand H_2L, *N*,*N*′-bis(3,5-di-*tert*-butylsalicylidene)-1,3-diaminobenzene yields a diferric complex, $[L_2Fe^{III}_2(NO_3)_2]$ (**1**), in which the d^5 high-spin iron(III) centers are ferromagnetically coupled through the spin polarization mechanism.

Introduction

The last two decades have witnessed an upsurge of studies related to magnetism with an aim to understand the phenomenon of exchange coupling.[1] Particularly, the designed synthesis of multinuclear complexes[2] exhibiting ferromagnetic exchange coupling has attracted the unabated interest of inorganic chemists. It involves a twofold challenge: (i) synthesis and (ii) control of the mechanism for the exchange coupling. Synthetic methods for both homo- and heterodinuclear complexes are about to reach the level of efficiency attained with mononuclear complexes.[3] A well-known strategy for bringing about ferromagnetic interactions in a compound is the so-called spin polarization of the electronic cloud of the species linking paramagnetic centers. The spin polarization mechanism is well-established in organic chemistry; ferromagnetic interactions are achieved by *m*-phenylene linkages of organic paramagnetic centers.[4] While the use of *m*-phenylene linkages to achieve parallel spin coupling in transition-metal complexes has indeed been successful in some cases,[2] antiferromagnetic interactions have also been reported.[5] Competing superexchange and spin polarization mechanisms and the orientation of the magnetic orbitals relative to the bridging ligand plane have accounted for these differences in the nature of the overall exchange interactions.

As a continuation of our ongoing project of using *m*-phenylenediamine[6] as a linker for generating dinucleating ligands, we have prepared the ligand H_2L (Scheme 1) and its diferric(III) complex, $[L_2Fe_2(NO_3)_2]$ (**1**), which exhibits ferromagnetic coupling through the spin polarization mechanism. To the best of our knowledge, this is the first example of a six-coordinate iron(III) compound in which the spins of the two ferric centers are parallel-oriented as a result of the spin polarization mechanism.

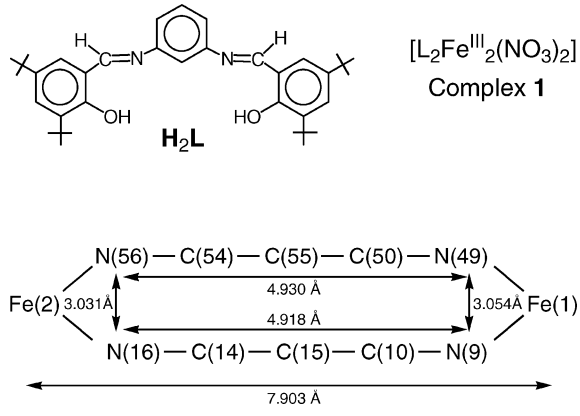

Scheme 1. The Schiff base ligand H_2L, *N*′,*N*-bis(3,5-di-*tert*-butylsalicylidene)-1,3-diaminobenzene and its Fe^{III} complex containing a 12-membered metallamacrocycle.

Results and Discussion

The reaction of $Fe(NO_3)_3{\cdot}9H_2O$ with the ligand H_2L in a 1:1 ratio in methanol yields the dinuclear complex $L_2Fe_2(NO_3)_2$ (**1**) as a dark green solid. By diffusion of hexane into a dichloromethane solution of **1**, X-ray quality crystals of $\mathbf{1}{\cdot}CH_2Cl_2{\cdot}C_6H_{12}$ were obtained (Figure 1).

[a] Max-Planck-Institute for Bioinorganic Chemistry,
Stiftstrasse 34-36, 45470 Mülheim an der Ruhr, Germany
Fax: +49-208-306-3951
E-mail: Chaudh@mpi-muelheim.mpg.de
Homepage: http://www.mpi-muelheim.mpg.de

Supporting information for this article is available on the WWW under http://www.eurjic.org or from the author.

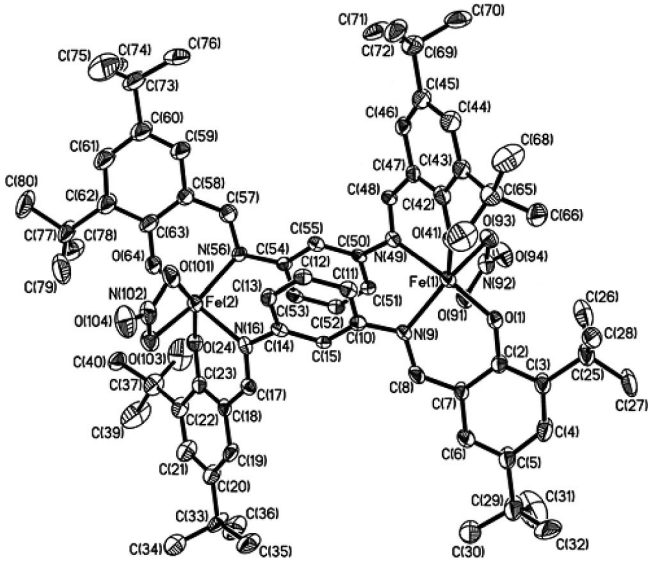

Figure 1. Molecular structure of $[L_2Fe_2(NO_3)_2]$ in **1**·CH_2Cl_2·C_6H_{12}. Selected bond lengths (in Å) and angles (in °): Fe(1)–O(41) 1.859(4), Fe(1)–O(1) 1.890(4), Fe(1)–N(9) 2.088(5), Fe(1)–O(93) 2.140(4), Fe(1)–O(91) 2.229(4), Fe(1)–N(49) 2.176(5), Fe(2)–O(24) 1.863(4), Fe(2)–O(64) 1.893(4), Fe(2)–N(56) 2.076(5), Fe(2)–O(103) 2.129(4), Fe(2)–N(16) 2.190(5), Fe(2)–O(101) 2.258(5), N(9)–Fe(1)–O(93) 158.5(2), O(1)–Fe(1)–N(49) 175.3(2), O(41)–Fe(1)–O(91) 152.4(2), N(56)–Fe(2)–O(103) 154.3(2), O(64)–Fe(2)–N(16) 176.4(2), O(24)–Fe(2)–O(101) 152.8(2).

The neutral molecule **1** contains two FeN_2O_4 hexacoordinate cores separated by the *m*-phenylene spacer. The coordination geometry at each iron ion is pseudo-octahedral, consisting, for example for the Fe(2) atom, of two oxygen atoms of a chelating nitrate ion, O(101), O(103), two phenolate oxygen atoms, O(64), O(24), and nitrogen atoms N(16) and N(56) from the *m*-phenylene linkers. The average values of the Fe–N and Fe–O distances agree well with those for high-spin ferric ions,[7] thus, the average bond lengths are 2.13 ± 0.06 Å for Fe–N, 1.88 ± 0.01 Å for Fe–O (phenoxide), and 2.19 ± 0.06 Å for Fe–O (nitrate).

The deprotonated ligand $[L]^{2-}$ acts in a bis(bidentate) fashion to generate a 12-membered metallamacrocycle $[Fe_2(\eta^2{:}\eta^2\text{-}L)_2]^{2+}$ unit (Scheme 1), the positive charge of which is neutralized by two chelating nitrate monoanions, which yields the neutral complex $[L_2Fe_2(NO_3)_2]$ (**1**). The *m*-phenylene linkers are almost parallel with a dihedral angle of only 1.1° between the two benzene planes and an average interplanar separation of 3.46 Å. Thus, an unusual nearly perfect, face-to-face π–π stacking interaction exists between the two aromatic rings; a ring carbon atom, for example C(55), lies just over another carbon atom, namely the C(12) of the other ring. Interestingly, the 1,3-positions of one benzene ring cannot be superimposed on those of the other ring. The Fe···Fe intramolecular distance is 7.90 Å, whereas the shortest *inter*molecular separation between the metals is 7.78 Å.

Inspection of the bond angles at the iron centers indicates that the ideal *trans*-positioned angles are O(1)–Fe(1)–N(49) [175.3(2)°] and O(64)–Fe(2)–N(16) [176.4(2)°], showing that the best equatorial planes for the iron centers are O(91)–O(93)–O(41)–N(9)–Fe(1) and O(101)–O(103)–O(24)–N(56)–Fe(2); the iron centers are displaced by only 0.0413 Å from these planes. These two equatorial planes are parallel to each other with a deviation of only 0.7°. That the iron basal planes are not perpendicular to the benzene planes is shown by the angle 125.4° between them. The nitrate ions occupy *cis* positions, as expected, of the equatorial planes for the iron centers, in an asymmetric bidentate (η^2) mode, as is shown by a long [Fe(1)–O(91) 2.229(4) Å] and a comparatively short [Fe(1)–O(93) 2.140(4) Å] bond length.

The zero-field Mössbauer spectrum of solid **1** at 80 K yields an isomer shift and quadrupole splitting, which are in complete accord with the d^5 high-spin nature of the ferric centers (δ = 0.55 mm s^{-1}, ΔE_Q = 1.16 mm s^{-1}).[8] The value for the quadrupole splitting is remarkably large in view of the fact that the d^5 configuration has no valence contribution to the electric field gradient. Presumably it reflects the ionic nature of iron–nitrate bonds in contrast to the covalence of the other ligands.

Magnetic susceptibility data measured for a polycrystalline sample of **1** at B = 1 T are displayed in Figure 2A as μ_{eff} per molecule vs. temperature. At 290 K, μ_{eff} is equal to 8.39 μ_B ($\chi_M \cdot T$ = 8.789 cm^3 K mol^{-1}), which is identical to the high-temperature limit expected for two magnetically weakly interacting iron(III) ions. Upon cooling, μ_{eff} continuously increases and reaches a maximum of 9.09 μ_B at

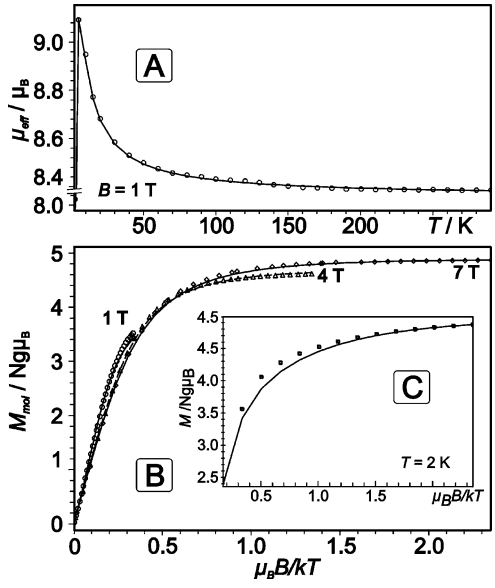

Figure 2. (A) Temperature dependence of the effective magnetic moment, μ_{eff}, of complex **1** recorded at B = 1 T, and (B) isofield measurements of the molar magnetization recorded at 1, 4, and 7 T with data sampling on a 1/T scale (variable-temperature-variable-field, VTVH). Inset (C) shows an isothermal magnetization measurement performed at 2 K. The solid lines in panels A–C are the result of a consistent spin Hamiltonian simulation with D_{Fe} = 0.9 cm^{-1}, g_{Fe} = 2.0, J = +0.195 cm^{-1}.

about 5 K ($\chi_M \cdot T$ = 10.335 $cm^3 K mol^{-1}$). This magnetic behavior is characteristic of ferromagnetic coupling between the adjacent iron(III) centers within the metallacycle in **1**.

Below 5 K, μ_{eff} drops to 8.02 μ_B at 2 K due to the combined effects of field saturation, exchange, and single-ion zero-field splitting. The corresponding properties of the ground-state spin manifolds were further probed by variable-temperature-variable-field (VTVH) measurements at 1, 4, and 7 T, with data sets sampled on a $1/T$ scale in the range 2–290 K (Figure 2B). The curves show decent nesting as a function of the field, which provides sensitive information on the parameters D and J. Simulation of the VTVH and $\mu_{eff}(T)$ data and global parameter optimization yields the values g_{Fe} = 2, D_{Fe} = 0.9 cm^{-1}, and J = +0.2 cm^{-1} for the single-ion g, axial zero-field splitting parameter, and the exchange coupling constant (with $\hat{H}_{ex} = -2J\ \hat{S}_1 \cdot \hat{S}_2$), respectively. No other parameters had to be invoked to obtain excellent fits (solid lines), particularly no TIP (temperature-independent paramagnetism) was necessary, or Θ_{Weiss} to account for intermolecular interactions. However, since we were not sure about possible covariances of D_{Fe} and J, we calculated a two-dimensional error surface as a function of the two parameters. The result, shown as a contour plot in Figure 3, nicely demonstrates the true global solution and rules out the presence of other local minima (the 3-D plot is depicted in Figure S1 in the Supporting Information). The range of confidence for the exchange coupling constant is safely estimated to be J = +0.2 (±0.05) cm^{-1}.

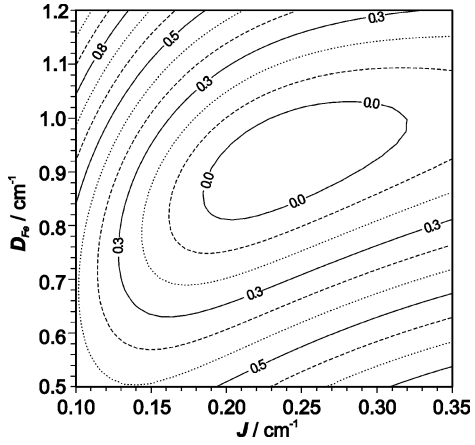

Figure 3. An error contour plot (in relative units) obtained for D_{Fe} and J values in the range 0.5–1.2 cm^{-1} and 0.1–0.35 cm^{-1}, respectively.

The nature of the magnetic ground-state levels of dimer **1** was also investigated "microscopically" by Mössbauer spectroscopy at liquid helium temperature with applied fields of 1–7 T (Figure 4). The hyperfine patterns show large magnetic splitting due to the presence of strong internal fields of about 51.6 T, as expected for monomeric ferric complexes, or ferromagnetically coupled dimers.[8] The large splitting particularly rules out again antiferromagnetic spin coupling, because that would generate nonmagnetic ground-state levels, so that components with small splitting only from the applied field would be superimposable on the inner part of the spectrum at v = ±2 $mm\,s^{-1}$. The persistent large splitting for all applied fields and the sharp peaks with a clear quadrupole shift (difference between peaks 1, 2 and 5, 6) indicate an "easy axis" of magnetization. This can be induced only by a sizeable zero-field interaction. Actually we had to introduce a rhombic contribution to the zero-field interaction, E/D = 0.3, to account for that magnetic anisotropy. (As is often the case, this term could not be resolved from the "macroscopic" SQUID magnetization data for the powder samples shown above.) The best values for the spin Hamiltonian parameters obtained from the corresponding simulations of the magnetic Mössbauer spectra are D_{Fe} = 0.8 (±0.15) cm^{-1} and J = +0.25 (±0.1) cm^{-1}, which are in nice accord with the SQUID result. Moreover, the magnetic hyperfine coupling constants obtained with the usual nuclear spin Hamiltonian (Equation S1 in the Supporting Information) for ^{57}Fe are $A/g_N\mu_N$ = (–21.6, –19.4, –20.9) T. We find the anisotropy of A relatively large for ferric ions, but this is in apparent accord with the large (positive) quadrupole splitting and results also from the anisotropy in the covalent bonds of the iron atom. From the magnetic spectra, the sign of the quadrupole interaction and asymmetry parameter (η = 0.2) of the electric field gradient tensor could also be determined (positive).

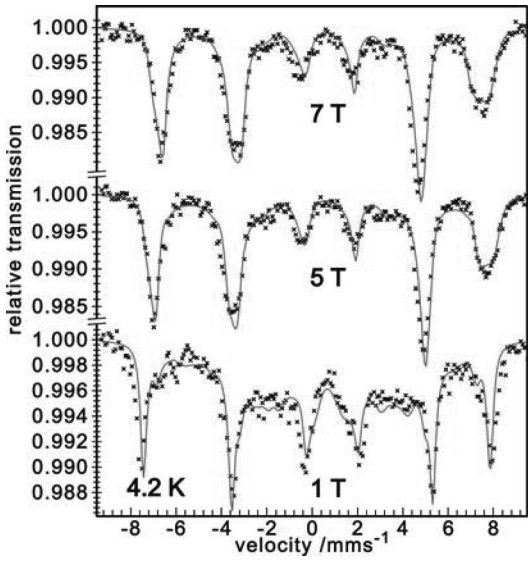

Figure 4. Mössbauer spectra of solid **1** recorded at 4.2 K with applied fields of 1, 5, and 7 T. The solid lines are obtained from spin Hamiltonian simulations as described in the text.

The zero-field splitting parameter, D_{Fe}, for iron(III) in **1** is larger than the ferromagnetic exchange coupling constant, J, of the dimer. This means that competing zero-field and exchange interactions mix the total spin manifolds, and thus, as such S_{total} and $M_{S,\,total}$ are no longer good quantum numbers. Therefore we refrain from describing our system as having an S_{total} = 5 ground state. The mixing of levels with crossings and avoided crossings for fields applied to our dimer in different directions is shown in several level plots given in the Supporting Information. We also note that a field-dependent magnetization measurement per-

formed at 2 K shows saturation at the level expected for an isolated ground state with S_{total} = 5 (Figure 2, inset C), but that should not be misinterpreted; since two weakly coupled or uncoupled spins of S_{Fe} = 5/2 exhibit the same behavior. In summary, the magnetic SQUID and Mössbauer measurements of **1** show unambiguously the ferromagnetic exchange interaction between two iron(III) centers with J = +0.2 (±0.05) cm^{-1}.

Stabilization of ferromagnetically coupled ground states is achieved through mechanisms dominated either by spin polarization or orthogonal magnetic orbitals. As the shortest *inter*molecular separation between iron centers in complex **1** is 7.78 Å, spin coupling devoid of any intervening atoms can be neglected. In other words, spin coupling occurs through the atoms joining the iron centers in the resulting metallacycle. As the iron basal planes are not perpendicular to the spacer *m*-phenylene rings and the intramolecular metal separation is as long as 7.90 Å, the ferromagnetic coupling observed in **1** cannot be attributed to the mechanism based on orbital symmetry. The remaining possibility, that is spin polarization effects, is thus the most probable mechanism for the spin coupling in **1**.

The spin polarization mechanism predicts a sign alternation of spin densities on adjacent bridging atoms of the ligand. We used the experimental geometry of **1** and performed density functional theory (DFT) calculations for the S = 5 high-spin state. We applied the Gaussian 03 suite of programs[9] and the unrestricted B3LYP[10] DFT scheme as activated by the Gaussian method keyword UB3LYP. The Fe and the directly attached O and N atoms were described by means of the triple zeta valence and polarization function (TZVP) basis set.[9,11] Thus, for all atoms directly involved in coordination, a rather flexible basis set has been used. The remaining C and H atoms have been treated by means of the split valence polarization (SVP)[9,11] and split valence (SV)[9,11] basis sets, respectively. For discussing the spin-density distribution, the atomic Mulliken spin densities have been considered (Figure 5). The largest spin density is computed for the iron atoms. The spin densities at the imine nitrogen atoms have the same sign as those at the iron atom, indicating spin delocalization toward the donor atoms. Given the topology (1,3-substitution) of the bridges, the spin densities at both iron atoms have the same sign, thus resulting in a net ferromagnetic exchange. The very weak nature of the coupling results from various competing exchange coupling paths arising from the highest number of unpaired electrons (five) possible for a transition-metal center and the path length of the intervening atoms involved.

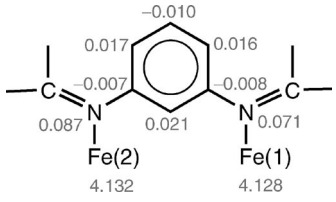

Figure 5. Spin-density distribution in the bridging atoms of **1** for the S = 5 state.

Conclusion

In summary, this work reports an unprecedented ferromagnetic spin coupling operating at a distance of 7.90 Å between two high-spin ferric centers through the spin polarization mechanism.

Experimental Section

H_2L: To a solution of 1,3-diaminobenzene (1.08 g; 10 mmol) in methanol (50 mL) was added 3,5-di-*tert*-butylsalicylaldehyde (4.65 g; 20 mmol) with stirring. The resulting mixture was heated under reflux for 2 h to yield a yellow precipitate, which was collected by filtration and recrystallized from acetone/water (9:1). Yield: 5.0 g (90%). M.p. 181–183 °C. EI-MS: *m*/*z* (%) = 540 (100) [M]$^+$, 525 (62.5) [M – CH_3]$^+$, 497 (13.6) [M – $C(CH_3)$]$^+$. ^{1}H NMR (CD_2Cl_2, 400 MHz): δ = 1.34 (s, 18 H, *t*Bu), 1.47 (s, 18 H, *t*Bu), 7.26–7.49 (m, 8 H, Ar), 8.75 (s, 2 H, HC=N) ppm. IR (KBr): $\tilde{\nu}$ = 3450, 2956, 2906, 2869, 1621, 1572, 1467, 1439, 1390, 1361, 1273, 1251, 1148, 965, 879, 770, 684, 643 cm^{-1}.

Complex 1, $[Fe_2L_2(NO_3)_2]$: A methanol solution of $Fe(NO_3)_3{\cdot}9H_2O$ (0.40 g, 1 mmol, 40 mL) and H_2L (0.54 g; 1 mmol) was heated under reflux for 1 h and yielded a green solution. On cooling, a green microcrystalline solid separated out. X-ray quality crystals in 75% yield grew over two days from a dichloromethane/hexane (2:1) solution. $CH_2Cl_2{\cdot}C_6H_{12}$ ($C_{79}H_{108}N_6O_{10}Cl_2Fe_2$) (1484.3): calcd. C 63.92, H 7.33, N 5.66, Fe 7.52; found C 64.6, H 7.0, N 5.7, Fe 7.7. MS-ES (pos.) (CH_2Cl_2): *m*/*z* (%) = 1250.7 (100) [M – NO_3]$^+$, 594–5 (≈ 90) [M – 2(NO_3)]$^{2+}$. MS-ESI (neg.) (CH_2Cl_2): *m*/*z* (%) = 1374.8 (100) [M + NO_3]. UV/Vis (CH_2Cl_2): λ_{max} (ε, M^{-1}cm^{-1}): 635 (11.4×10^3), 367 (32.0×10^3) nm. IR (KBr): $\tilde{\nu}$ = 2959, 2902, 2868, 1609, 1577, 1534, 1483, 1462, 1424, 1384, 1272, 1254, 1175, 964, 870, 849, 834, 781, 748, 693, 539 cm^{-1}.

Crystal Data for a $1{\cdot}CH_2Cl_2{\cdot}C_6H_{12}$: Formula: $C_{79}H_{108}Cl_2Fe_2N_6O_{10}$, fw = 1484.31, T = 100(2) K, monoclinic, space group $P2_1/c$, a = 30.004(3) Å, b = 20.167(2) Å, c = 13.5983(9) Å, β = 90.951(6)°, V = 8227.1(13) Å^3, Z = 4, D_c = 1.198 Mg/m^3, μ (Mo-K_α) = 0.474 mm^{-1}. Data were corrected for Lorentzian and polarization effects. No absorption correction; 82051 reflections were collected, of which 10735 [R(int) = 0.1418] were considered as unique. The structure was solved by direct methods with SHELXS-97 and refined by using the full-matrix least-squares method on F^2 using SHELXL-97.[12] The hydrogen atoms were located from a difference synthesis and refined with isotropic thermal parameters. Hexane and dichloromethane solvent molecules in **1** were found to be severely disordered. There are two positions in the asymmetric unit which are occupied by a mixture of these two solvents. Position 1 was refined with an 0.5 occupation of hexane (C201–C206) and two split positions of CH_2Cl_2 with occupancies of 0.31 (C200) and 0.19 (C215). The disorder of position 2 was treated with an 0.5:0.5 occupation of hexane (C301–C306) and dichloromethane (C300). C–Cl and C–C distances were restrained to be equal within errors, and equal displacement parameters were refined for the corresponding atoms by using the DFIX, SADI, and EADP instructions of SHELXL-97. A total of 47 restraints was used. Refinement of 911 parameters with 47 restraints with anisotropic thermal parameters for all non-hydrogen atoms gave $R_1[I>2\sigma(I)]$ = 0.0754, R_1 (all data) = 0.1517 and goodness-of-fit on F^2 = 1.067.

CCDC-676360 contains the supplementary crystallographic data for this paper. These data can be obtained free of charge from the

Cambridge Crystallographic Data Centre via www.ccdc.cam.ac.uk/data_request/cif.

Supporting Information (see footnote on the first page of this article): Details of the magnetic SQUID and Mössbauer spectroscopic measurements together with the spin Hamiltonian simulations are given.

Acknowledgments

This work was supported by the Deutsche Forschungsgemeinschaft (Priority Program: "Molecular Magnetism", Bi-380/6-3; Ch111/3-3). Thanks are due to H. Schucht, A. Göbels, B. Mienert, and F. Reikowski for skillful technical assistance.

[1] O. Kahn, *Molecular Magnetism*, Wiley-VCH, Weinheim, Germany, **1993**.

[2] Selected examples: a) V. A. Ung, A. M. W. Cargill Thompson, D. A. Bardwell, D. Gatteschi, J. C. Jeffery, J. A. McCleverty, F. Totti, M. D. Ward, *Inorg. Chem.* **1997**, *36*, 3447; b) T. Ishida, S. Mitsubori, T. Nogami, N. Takeda, M. Ishikawa, H. Iwamura, *Inorg. Chem.* **2001**, *40*, 7059; c) X. Ottenwaelder, J. Cano, Y. Journaux, E. Riviére, C. Brennan, M. Nierlich, R. Ruiz-García, *Angew. Chem. Int. Ed.* **2004**, *43*, 850; d) M. Pascu, F. Lloret, N. Avarvari, M. Julve, M. Andruh, *Inorg. Chem.* **2004**, *43*, 5189; e) T. Glaser, M. Heidemeier, S. Grimme, E. Bill, *Inorg. Chem.* **2004**, *43*, 5192; f) F. Lloret, G. De Munno, M. Julve, J. Cano, R. Ruiz, A. Caneshi, *Angew. Chem. Int. Ed.* **1998**, *37*, 135; g) E. Pardo, K. Bernot, M. Julve, F. Lloret, J. Cano, R. Ruiz-García, F. S. Delgado, C. Ruiz-Perez, X. Ottenwaelder, Y. Journaux, *Angew. Chem. Int. Ed.* **2004**, *43*, 2768; h) E. Pardo, J. Faus, M. Julve, F. Lloret, M. C. Munoz, J. Cano, X. Ottenwaelder, Y. Journaux, R. Carrasco, G. Blay, I. Fernandez, R. Ruiz-Garcia, *J. Am. Chem. Soc.* **2003**, *125*, 10770; i) A. R. Paital, T. Mitra, D. Ray, W. T. Wong, J. Ribas-Arino, J. J. Novoa, J. Ribas, G. Aromí, *Chem. Commun.* **2005**, 5172; j) I. Fernandez, R. Ruiz, J. Faus, M. Julve, F. Lloret, J. Cano, X. Ottenwaelder, Y. Journaux, M. Carmen Munoz, *Angew. Chem. Int. Ed.* **2001**, *40*, 3039.

[3] See for example: a) P. Chaudhuri, *Coord. Chem. Rev.* **2003**, *243*, 143; b) H. Okawa, H. Furutachi, D. E. Fenton, *Coord. Chem. Rev.* **1998**, *174*, 51; c) P. A. Figato, S. Tamburini, *Coord. Chem. Rev.* **2004**, *248*, 1717.

[4] a) J. C. Longuet-Higgins, *J. Chem. Phys.* **1950**, *18*, 265; b) H. Iwamura, *Adv. Phys. Org. Chem.* **1990**, *26*, 179; c) A. Rajca, *Chem. Rev.* **1994**, *94*, 871.

[5] a) E. F. Hasty, L. J. Wilson, D. N. Hendrickson, *Inorg. Chem.* **1978**, *17*, 1834; b) T. Ishida, T. Kawakami, S. Mitsubori, T. Nogami, K. Yamaguchi, H. Iwamura, *J. Chem. Soc., Dalton Trans.* **2002**, 3177; c) M. Matsushita, T. Yasuda, R. Kawano, T. Kawai, T. Iyoda, *Chem. Lett.* **2000**, 812; d) H. Torayama, T. Nishida, H. Asada, M. Fujiwara, T. Matsushita, *Polyhedron* **1997**, *16*, 3787; e) A. Dei, D. Gatteschi, C. Sangregorio, L. Sorace, M. G. F. Vaz, *Inorg. Chem.* **2003**, *42*, 1701; f) A. Mederos, S. Dominguez, R. Hernández-Molina, J. Sanchiz, F. Brito, *Coord. Chem. Rev.* **1999**, *193–195*, 857 and references cited therein.

[6] a) S. Mukherjee, E. Rentschler, T. Weyhermüller, K. Wieghardt, P. Chaudhuri, *Chem. Commun.* **2003**, 1828; b) S. Mukherjee, T. Weyhermüller, E. Bothe, K. Wieghardt, P. Chaudhuri, *Dalton Trans.* **2004**, 3842.

[7] a) F. A. Cotton, G. Wilkinson, C. A. Murillo, M. Bochmann, *Advanced Inorganic Chemistry*, 6th ed., Wiley-Interscience, New York, NY, **1999**; b) G. Wilkinson, R. D. Gillard, J. A. McCleverty (Eds.), *Comprehensive Coordination Chemistry*, Pergamon Press, Oxford, **1987**.

[8] A. X. Trautwein, E. Bill, E. L. Bominaar, H. Winkler, *Structure Bonding* **1991**, *78*, 1.

[9] M. J. Frisch, G. W. Trucks, H. B. Schlegel, G. E. Scuseria, M. A. Robb, J. R. Cheeseman, J. A. Montgomery Jr, T. Vreven, K. N. Kudin, J. C. Burant, J. M. Millam, S. S. Iyengar, J. Tomasi, V. Barone, B. Mennucci, M. Cossi, G. Scalmani, N. Rega, G. A. Petersson, H. Nakatsuji, M.Hada, M. Ehara, K. Toyota, R. Fukuda, J. Hasegawa, M. Ishida, T. Nakajima,Y. Honda, O. Kitao, H. Nakai, M. Klene, X. Li, J. E. Knox, H. P. Hratchian, J. B. Cross, C. Adamo, J. Jaramillo, R. Gomperts, R. E. Stratmann, O. Yazyev, A. J. Austin, R. Cammi, C. Pomelli, J. W. Ochterski, P. Y. Ayala, K. Morokuma, G. A. Voth, P. Salvador, J. J. Dannenberg, V. G. Zakrzewski, S. Dapprich, A. D. Daniels, M. C. Strain, O. Farkas, D. K. Malick, A. D. Rabuck, K. Raghavachari, J. B. Foresman, J. V. Ortiz, Q. Cui, A. G. Baboul, S. Clifford, J. Cioslowski, B. B. Stefanov, G. Liu, A. Liashenko, P. Piskorz, I. Komaromi, R. L. Martin, D. J. Fox, T. Keith, M. A. Al-Laham, C. Y. Peng, A. Nanayakkara, M. Challacombe, P. M. W. Gill, B. Johnson, W. Chen, M. W. Wong, C. Gonzalez, J. A. Pople, *Gaussian 03*, Revision C.01, Gaussian, Inc., Wallingford CT, **2004**.

[10] A. D. Becke, *J. Chem. Phys.* **1993**, *98*, 5648; C. Lee, W. Yang, R. G. Parr, *Phys. Rev. B* **1988**, *37*, 785; B. Miehlich, A. Savin, H. Stoll, H. Preuss, *Chem. Phys. Lett.* **1989**, *157*, 200.

[11] A. Schaefer, H. Horn, A. Ahlrichs, *J. Chem. Phys.* **1992**, *97*, 2571; A. Schaefer, C. Huber, R. Ahlrichs, *J. Chem. Phys.* **1994**, *100*, 5829.

[12] a) *SHELXTL*, Version 5, Siemens Analytical X-ray Instruments, Inc. **1994**; b) G. M. Sheldrick, University of Göttingen, Göttingen, Germany **1997**.

Received: March 11, 2008
Published Online: April 4, 2008

